Pharmaceutical Research, Vol. 24, No. 11, November 2007 (© 2007)
DOI: 10.1007/s11095-007-9415-0

Research Paper

Endocytosis and Interaction of Poly (Amidoamine) Dendrimers with Caco-2 Cells

Kelly M. Kitchens,[1] Amy B. Foraker,[1] Rohit B. Kolhatkar,[1] Peter W. Swaan,[1] and Hamidreza Ghandehari[1,2]

Received July 3, 2007; accepted July 16, 2007; published online August 15, 2007

Purpose. To investigate the internalization and subcellular trafficking of fluorescently labeled poly (amidoamine) (PAMAM) dendrimers in intestinal cell monolayers.
Materials and methods. PAMAM dendrimers with positive or negative surface charge were conjugated to fluorescein isothiocyanate (FITC) and visualized for colocalization with endocytosis markers using confocal microscopy. Effect of concentration, generation and charge on the morphology of microvilli was observed using transmission electron microscopy.
Results. Both cationic and anionic PAMAM dendrimers internalized within 20 min, and differentially colocalized with endocytosis markers clathrin, EEA-1, and LAMP-1. Transmission electron microscopy analysis showed a concentration-, generation- and surface charge-dependent effect on microvilli morphology.
Conclusion. These studies provide visual evidence that endocytic mechanism(s) contribute to the internalization and subcellular trafficking of PAMAM dendrimers across the intestinal cells, and that appropriate selection of PAMAM dendrimers based on surface charge, concentration and generation number allows the application of these polymers for oral drug delivery.

KEY WORDS: Caco-2 cells; intracellular trafficking; oral drug delivery; poly (amidoamine) dendrimers.

INTRODUCTION

Poly (amidoamine) (PAMAM) dendrimers are a class of water-soluble polymers that have demonstrated potential use as oral drug delivery carriers (1–3). These macromolecular structures have a unique architecture, in which branching occurs with an exponential increase of amidoamine groups (4). Each consecutive series of the branching step is termed a generation (G) and dendrimer size and number of surface groups increase with each successive generation. In general, "full generation" PAMAM dendrimers are terminated with amine surface groups (e.g. G1, G2, etc.) whereas "half generation" dendrimers are terminated with carboxylate (e.g. G1.5, G2.5, etc.). The branching multiplicity of dendrimers allows for therapeutic agents to be encapsulated in the interior void spaces, or conjugated to their surface groups (4). Importantly, PAMAM dendrimers are capable of traversing the intestinal epithelial barrier (3,5–8) and may allow a drug to bypass the P-gp efflux system, (9) thereby rendering the dendrimer system uniquely suitable for applications in oral drug delivery. To this end, we have previously reported the transport and cytotoxicity profiles of PAMAM dendrimers across epithelial cell monolayers (5,6,8,10). Visual evidence suggested that PAMAM dendrimers of appropriate surface charge and concentration may open the tight junctions of apposing cells (8). Interestingly, transepithelial transport of PAMAM dendrimers demonstrated a combination of para-and transcellular pathways, while temperature-dependent studies of cationic dendrimers suggested the contribution of an energy-dependent process such as endocytosis (11). To definitively corroborate and extend these indirect observations, the present study utilized confocal laser scanning microscopy (CLSM) to record intracellular trafficking and spatial localization of dendrimers in Caco-2 cells. The extent of colocalization of PAMAM dendrimers with established endocytosis markers provides the first mechanistic evidence of dendrimer cell entry.

Another important consideration for the use of PAMAM dendrimers in oral drug delivery is their biocompatibility. As we have noted previously, the viability of Caco-2 cells in the presence of PAMAM dendrimers depends on surface charge, concentration, generation and incubation time (5,6). These studies were conducted using standard cytotoxicity assays and provided an initial guideline for screening the transepithelial transport of PAMAM dendrimers. However, the mechanistic details behind PAMAM dendrimer cytotoxicity are poorly understood. Thus, the present study employed transmission electron microscopy

[1] Center for Nanomedicine and Cellular Delivery, Department of Pharmaceutical Sciences, University of Maryland School of Pharmacy, 20 Penn Street, HSFII-Room 625, Baltimore, Maryland 21201-1075, USA.
[2] To whom correspondence should be addressed. (e-mail: hghandeh@rx.umaryland.edu)

ABBREVIATIONS: FITC, fluorescein isothiocyanate; G, generation; HBSS, hank's balanced salt solution; PAMAM, poly (amidoamine).

(TEM) to examine the morphological changes on the apical surface of Caco-2 cells upon incubation with PAMAM dendrimers of different surface chemistry, size, and donor concentration. These studies provide the first step towards elucidating dendrimer-induced cytotoxicity and aid the selection of biocompatible PAMAM dendrimers for subsequent *in vivo* application.

MATERIALS AND METHODS

Materials. PAMAM dendrimer solutions ($G2NH_2$, $G4NH_2$, G1.5COOH, G3.5COOH) and fluorescein isothiocyanate (FITC) were purchased from Sigma-Aldrich (St. Louis, MO). Caco-2 cells were purchased from American Type Culture Collection (Rockville, MD). Transferrin fluorescein conjugate, Alexa Fluor® 568 goat anti-mouse IgG, and cell culture reagents were purchased from Invitrogen (Carlsbad, CA). Primary antibodies against clathrin heavy chain, a 180 kDa subunit of clathrin, early endosomal antigen 1 (EEA-1), and lysosome-associated membrane protein 1 (LAMP-1), a 120 kDa heavily glycosylated lysosomal integral membrane protein (12), were purchased from Affinity Bioreagents (Golden, CO). All other solvents and reagents were purchased from Sigma-Aldrich unless otherwise noted.

Fluorescent Labeling of PAMAM Dendrimers. PAPAMAM dendrimers were fluorescently labeled as previously described (8). Briefly, $G2NH_2$ and G1.5COOH were conjugated to FITC at a feed molar ratio of 1:1. Fluorescently labeled PAMAM dendrimers were purified by dialysis against distilled water using dialysis membranes of 500 MWCO (Spectrum Laboratories, Inc., Rancho Dominguez, CA). They were then fractionated on a Superose 12 HR 16/50 preparative column using a Fast Protein Liquid Chromatography (FPLC) system (Amersham Pharmacia Biotech, Uppsala, Sweden) with a mobile phase of 30/70% (v/v) acetonitrile:Tris buffer (pH 8.0) at a flow rate of 1.0 ml/min. Fractions corresponding to the appropriate dendrimer size and molecular weight were collected, dialyzed against distilled water, and lyophilized. The extent of FITC labeling was measured using an Ultrospec 4000 UV-vis spectrophotometer (Biochrom Ltd., Cambridge, UK) at the wavelength of 495 nm.

Caco-2 Cell Culture. Caco-2 cells (passages 30–60) were grown at 37°C in an atmosphere of 5% CO_2 and 95% relative humidity. Cells were maintained in T-75 flasks using Dulbecco's Modified Eagle's Medium supplemented with 10% fetal bovine serum, 1% non-essential amino acids, 10,000 units/ml penicillin, 10,000 μg/ml streptomycin and 25 μg/ml amphotericin. Growth medium was changed every 2 days. Cells were passaged at 70–90% confluency using 0.25% trypsin/ethylenediamine tetraacetic acid (EDTA) solution.

Immunofluorescence. Caco-2 cells were seeded at 30,000 cells/cm^2 onto collagen-coated 4-chamber culture slides (BD Biosciences, Bedford, MA), maintained under normal incubation conditions and used for transport experiments 3–5 days post-seeding. Growth medium was replaced with phosphate-buffered saline (PBS), and cells were equilibrated with PBS for 30 min. Cells were treated with 300 μl transferrin fluorescein (250 μg/ml) for 1 h at 4°C and were then chased with 300 μl PBS at 37°C for 30 min. For dendrimer internalization, cells were incubated with 300 μl of PAMAM-FITC samples (100 nM) for 20 and 60 min at 37°C after which the dendrimers were removed by washing the cells three times with PBS. The cells were fixed with 300 μl paraformaldehyde (4%) for 20 min at room temperature and permeabilized using 0.2% Triton X-100 in blocking solution, made of 1% (w/v) bovine serum albumin (BSA) in PBS, for 20 min. Cells were incubated with 300 μl BSA/PBS (1%) for 30 min. After removing the blocking solution cells were incubated with 300 μl of primary antibodies anti-clathrin (6 μg/ml), anti-EEA-1 (4 μg/ml), and anti-LAMP-1 (5 μg/ml) for 20 and 60 min at room temperature. After removal of the primary antibody, cells were washed three times with 1% BSA/PBS and incubated with 300 μl Alexa Fluor® 568 goat anti-mouse IgG (10 μg/ml) for 1 h at room temperature. Then cells were washed with PBS, and the chambers removed. Gel/Mount (Biomeda Corp., Foster City, CA) was added to each region and slides were covered with a glass coverslip, sealed, and dried overnight at 4°C.

Confocal Microscopy. Images were obtained using a Nikon Eclipse TE2000 inverted CLSM (Nikon Instruments, Inc., Melville, NY), equipped with an argon laser. FITC was visualized with excitation and emission wavelengths of 488 and 515 nm, respectively; Alexa Fluor® 568 was visualized with excitation and emission wavelengths of 543 nm and 605 nm, respectively. The 3-D confocal images were acquired using the following settings of the Nikon EZ-C1 acquisition software (version 2.3, Image systems, Inc., Columbia, MD): 60× oil objective with numerical aperture=1.4; 100 μm pinhole size; 8.64 μs scan dwell; 512×512 pixel size; 0.40 μm z-step size. Confocal images were processed using Volocity 3.5.1 3D imaging software (Improvision, Inc., Lexington, MA) by applying iterative deconvolution using a calculated point spread function for each channel. The extent of colocalization was determined using the software's session arithmetic function, in which the colocalization coefficient (M_x) was calculated by the following equation:

$$M_x = \frac{\sum_i \chi_{i,\,\mathrm{coloc}}}{\sum_i \chi_i} \tag{1}$$

where $x_{i,\mathrm{coloc}}$ is the value of voxel i of the overlapped FITC and Alexa Fluor 568® components, and x_i is the value of voxel i of the FITC component (13).

The Pearson's correlation coefficient (r) was measured to describe the correlation between the intensity distributions of FITC and Alexa Fluor 568® components with the following equation:

$$r = \frac{\sum_i (x_i - x_{\mathrm{aver}}) \cdot (y_i - y_{\mathrm{aver}})}{\sqrt{\left[\sum_i (x_i - x_{\mathrm{aver}})^2 \cdot (y_i - y_{\mathrm{aver}})^2\right]}} \tag{2}$$

where x_i and y_i are the values of voxel i of the FITC and Alexa Fluor 568® components, respectively (13). Each colocalized image had r values between 0 to 1 (data not shown), which indicates a positive correlation between FITC and Alexa Fluor 568® signals.

Transmission Electron Microscopy. Caco-2 cells were seeded at 80,000 cells/cm^2 onto polycarbonate 12-well

Transwell® filters of 3.0 μm mean pore size and 1.0 cm^2 surface area (Corning Incorporated, Corning, NY). The cells were maintained under incubation conditions described above and used for transport experiments 21–28 days post-seeding. Upon confluency, cells were washed two times with PBS, and incubated with 0.5 ml PAMAM dendrimers for 2 h. The cells were washed three times with ice-cold PBS to remove the dendrimer solutions, and the filters were excised and fixed with 4% formaldehyde/1% glutaraldehyde in buffer. Cells were post-fixed in 1% osmium tetroxide. After en bloc staining with aqueous 2% uranyl acetate, cells were dehydrated in a graded series of ethanol washes, embedded in Spurr's resin and polymerized. Ultrathin sections were stained with uranyl acetate and lead citrate and examined on a Zeiss 10 CA electron microscope at 60 kV accelerating voltage.

RESULTS AND DISCUSSION

To further elucidate the cellular entry and intracellular trafficking mechanism of PAMAM dendrimers we recorded the spatial and temporal intracellular localization in Caco-2 cells using CLSM. When grown to confluence, this cell line forms monolayers of absorptive enterocytes that differentiate into polarized, columnar cells representative of the small intestinal epithelium exhibiting well-developed microvilli and tight junctions (14). Caco-2 cells express a polarized distribution of metabolically active enzymes, including alkaline phosphatase and several cytochrome P450s and peptidases (15). Due to these characteristics, Caco-2 cell monolayers were used as an *in vitro* model reflective of the oral absorption potential of PAMAM dendrimers in humans (16,17). Dendrimers were fluorescently labeled with FITC at 1:1 feed molar ratios to facilitate recording their subcellular trafficking and intracellular localization upon cell entry. Upon labeling, the PAMAM-FITC conjugates had resultant molar ratios of 1:1.3 ($G2NH_2$:FITC) and 1:0.1 (G1.5COOH:FITC). Transferrin, a positive control for early and receptor recycling compartments (18), showed distinct perinuclear staining after 20 min incubation (Fig. 1). Significant colocalization (M_x 80.3%, Table I) between transferrin and clathrin occurred as early as 20 min as demonstrated by the overlap in FITC and Alexa Fluor 568® channels (Fig. 1). Similarly, we

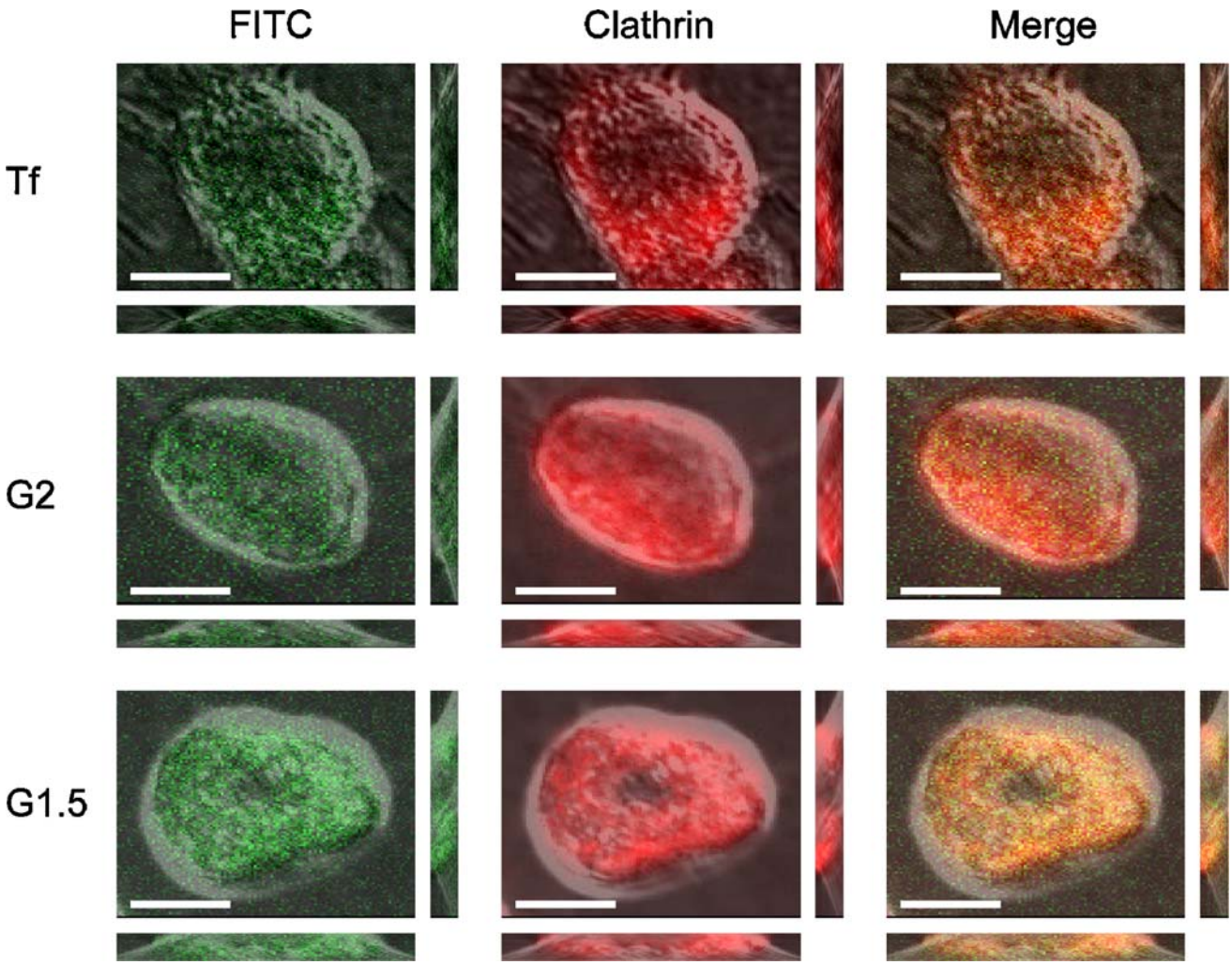

Fig. 1. Internalization of fluorescently labeled transferrin (250 μg/ml) and PAMAM dendrimers (100 nM) in Caco-2 cells. The orange color in merged panels indicates colocalization with clathrin heavy chain after 20 min. *Main panels* illustrate the *xy* plane; *vertical panels* illustrate the *yz* plane; *horizontal panels* illustrate the *xz* plane. Scale bars=5 μm.

Table I. Extent of Colocalization Between Transferrin and PAMAM Dendrimers with Endocytosis Markers[a]

	Incubation Time (min)	Clathrin	EEA-1	LAMP-1
Transferrin	20	80.3±3.1%	70.4±7.0%	63.9±7.3%
	60	83.4±0.2%	79.6±0.4%	57.0±8.6%
$G2NH_2$	20	74.3±5.2%	76.7±3.4%	37.4±5.9%
	60	73.7±3.8%	72.1±0.4%	59.0±5.2%
G1.5COOH	20	70.8±3.9%	60.1±6.8%	58.7±2.0%
	60	75.3±1.2%	53.8±9.7%	48.9±1.3%

[a] Colocalization coefficients (M_x) were calculated using Eq. 1. M_x values are reported as mean±standard error of the mean (n=6).

observed perinuclear staining of FITC-labeled PAMAM dendrimers and significant colocalization coefficients with clathrin (Fig. 1, Table I). Since clathrin serves as a hallmark endocytosis marker that aids in the formation of a coated pit upon membrane invagination (19), these studies provide direct evidence that PAMAM dendrimers may be internalized through a "classical" clathrin-dependent receptor-mediated endocytosis process.

Transferrin colocalized with the lysosomal marker protein, LAMP-1, to a significantly lower extent as compared with clathrin (Fig. 2, M_x 63.9%). Although LAMP-1 is predominantly located in the lysosomes, LAMP proteins are not confined solely to these compartments and may be detected in endosomes as well (20). This may explain the colocalization observed between transferrin, a typical marker for early endosomes, and LAMP-1. $G2NH_2$ and G1.5COOH displayed some colocalization with LAMP-1 after 20 min (Fig. 2), with M_x values of 37.3 and 58.7%, respectively (Table I). This lower degree of colocalization with LAMP-1 further demonstrates that dendrimers are localized primarily in early endosomal compartments. To determine whether these results are dependent on incubation time, identical

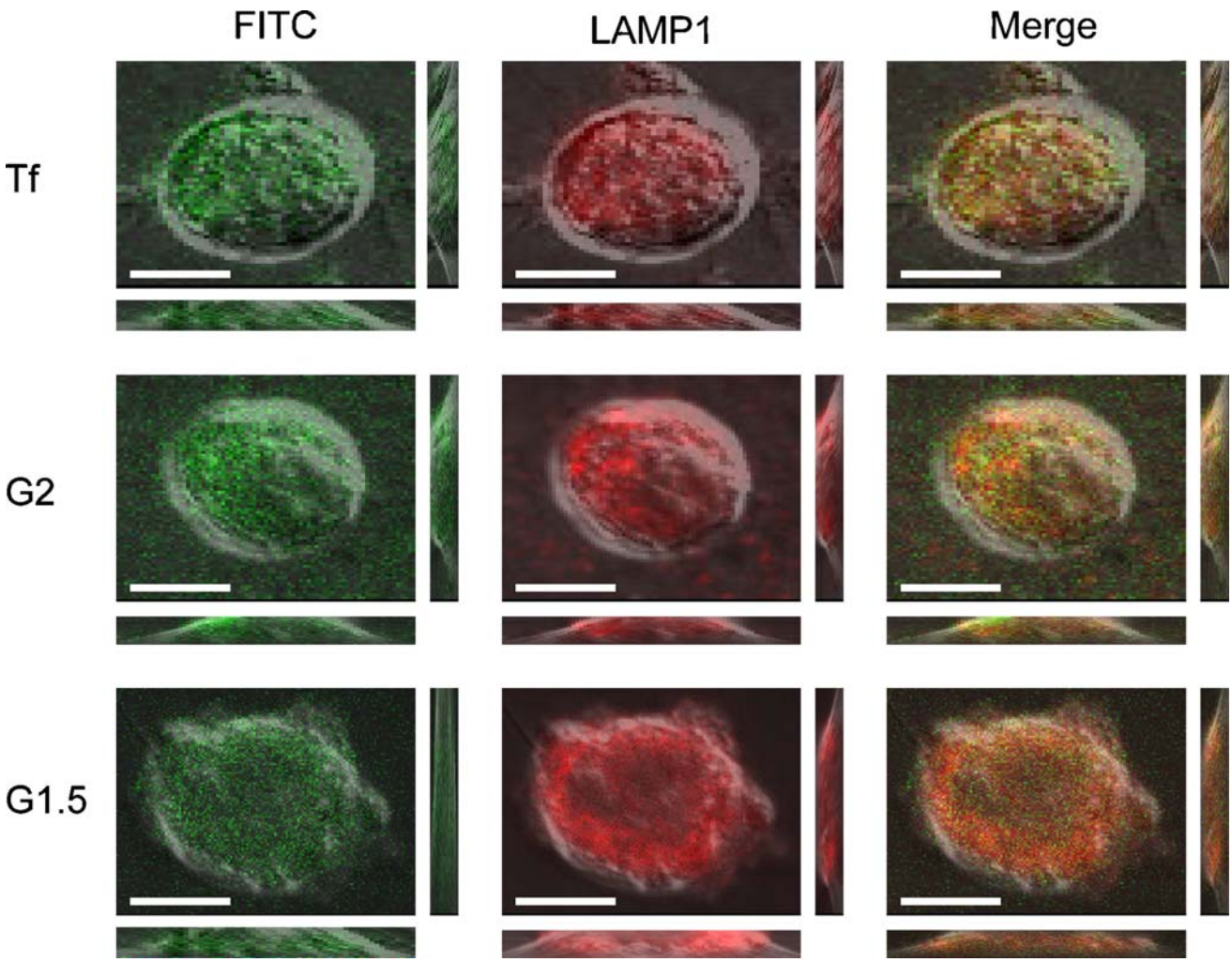

Fig. 2. Internalization of fluorescently labeled transferrin (250 μg/ml) and PAMAM dendrimers (100 nM) in Caco-2 cells. The *orange* color in merged panels indicates colocalization with lysosome-associated membrane protein 1 (LAMP-1) after 20 min. *Main panels* illustrate the *xy* plane; *vertical panels* illustrate the *yz* plane; *horizontal panels* illustrate the *xz* plane. Scale bars=5 μm.

experiments were performed using a 60-min chase. There were no changes observed in colocalization between clathrin and transferrin, which was anticipated since transferrin is internalized with its receptor, followed by rapid recycling of the apotransferrin-receptor complex to the cell membrane from early endosomes (21). Similarly, clathrin colocalization with $G2NH_2$ and G1.5COOH remained virtually unaltered after 60-min treatment (Fig. 3a, Table I). Thus, PAMAM dendrimers maintained a high degree of colocalization with clathrin irrespective of incubation time, indicating the constant presence of dendrimers in early endosomes. We observed insignificant changes in the lysosomal localization of transferrin and PAMAM dendrimers after 60 min (Fig. 3b). Interestingly, colocalization of $G2NH_2$ with LAMP-1 increased proportionally with time, suggesting lysosomal trafficking of cationic dendrimers is incubation time-dependent.

EEA-1 is a membrane-bound protein component (160 kDa) specific to early endosomes essential for fusion between early endocytic vesicles (22,23). The colocalization between this marker protein and transferrin was 70.4% (Table I). $G2NH_2$ and G1.5COOH colocalized with EEA-1, 76.7 and 60.1% after 20 min, respectively (Fig. 4), which reduced over time (M_x=72.1 and 53.8% after 60 min, respectively). Overall, the extent of G1.5COOH colocalization with LAMP-1 was almost twice the extent of colocalization between $G2NH_2$ and LAMP-1, although this differential declined after 60 min. These observations suggest that G1.5COOH may partition out of endosomes and have greater accumulation in lysosomes than $G2NH_2$ at early incubation times. In the acidic pH of secondary endosomes and lysosomes, G1.5COOH would have a net cationic potential through the secondary amine groups to interact with the negatively charged membrane, which could explain the appreciable partitioning and accumulation of these dendrimers

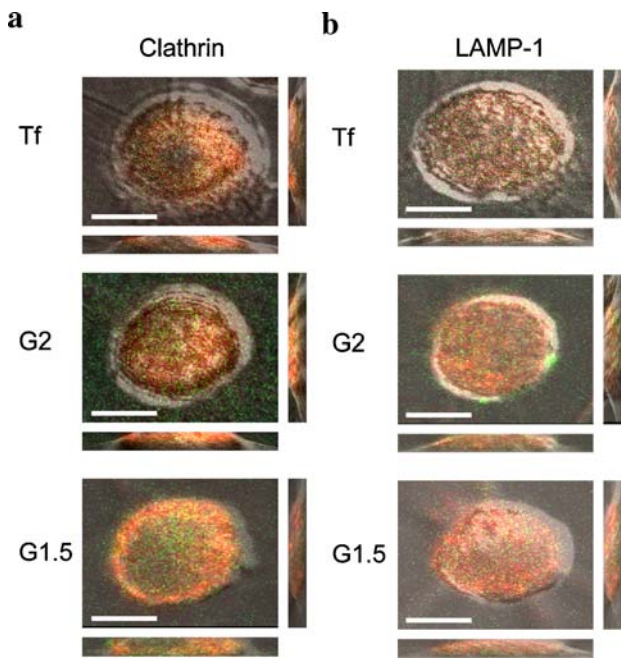

Fig. 3. Colocalization of fluorescently labeled transferrin and PAMAM dendrimers with **a** clathrin heavy chain and **b** LAMP-1 after 60 min. Scale bars=5 μm.

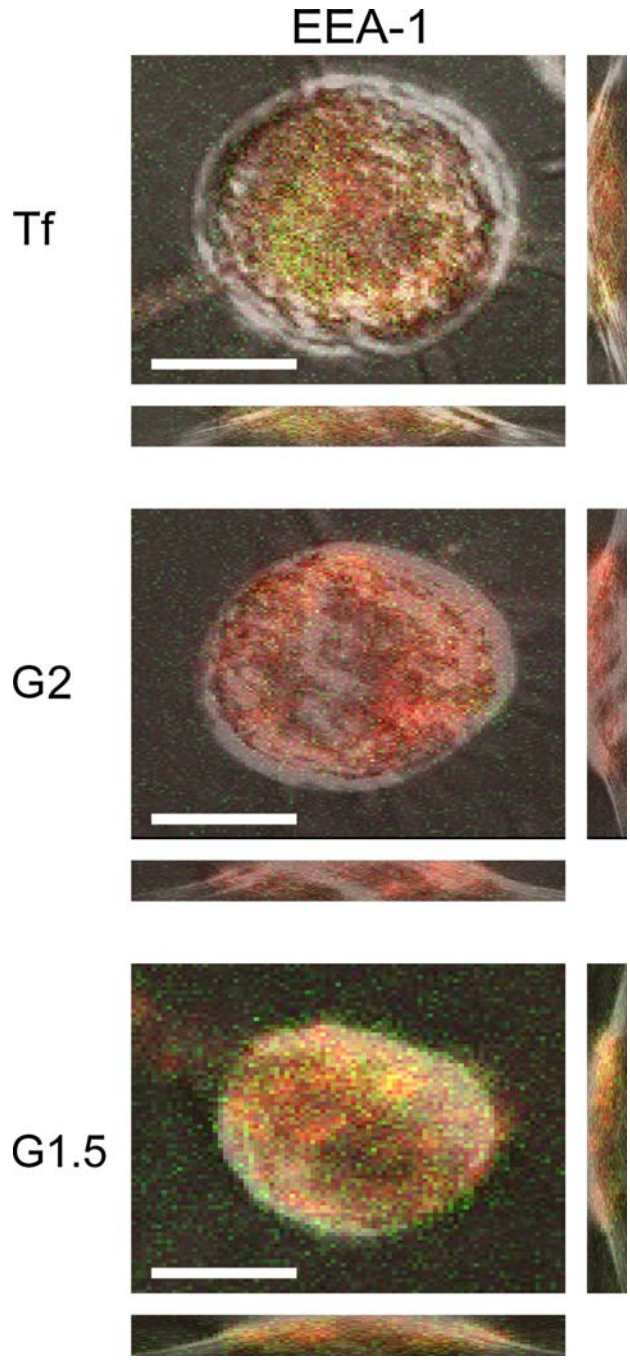

Fig. 4. Colocalization of fluorescently labeled transferrin and PAMAM dendrimers with early endosomal antigen 1 (EEA-1) after 20 min. Scale bars=5 μm.

out of endosomes and into lysosomal compartments, respectively. After longer incubation times, we observed increased localization of $G2NH_2$ in lysosomal compartments. PAMAM-NH_2 dendrimers are protonated at the physiological pH of the intracellular environment, which promotes lysosomal membrane permeability of cationic dendrimers into these compartments. Overall, the confocal data provide visual evidence that PAMAM dendrimers, both cationic and anionic, are localized in endosomal compartments, and dendrimer trafficking to secondary endosomes and lysosomes is dependent on time and dendrimer surface charge. This data demonstrates dendrimer-

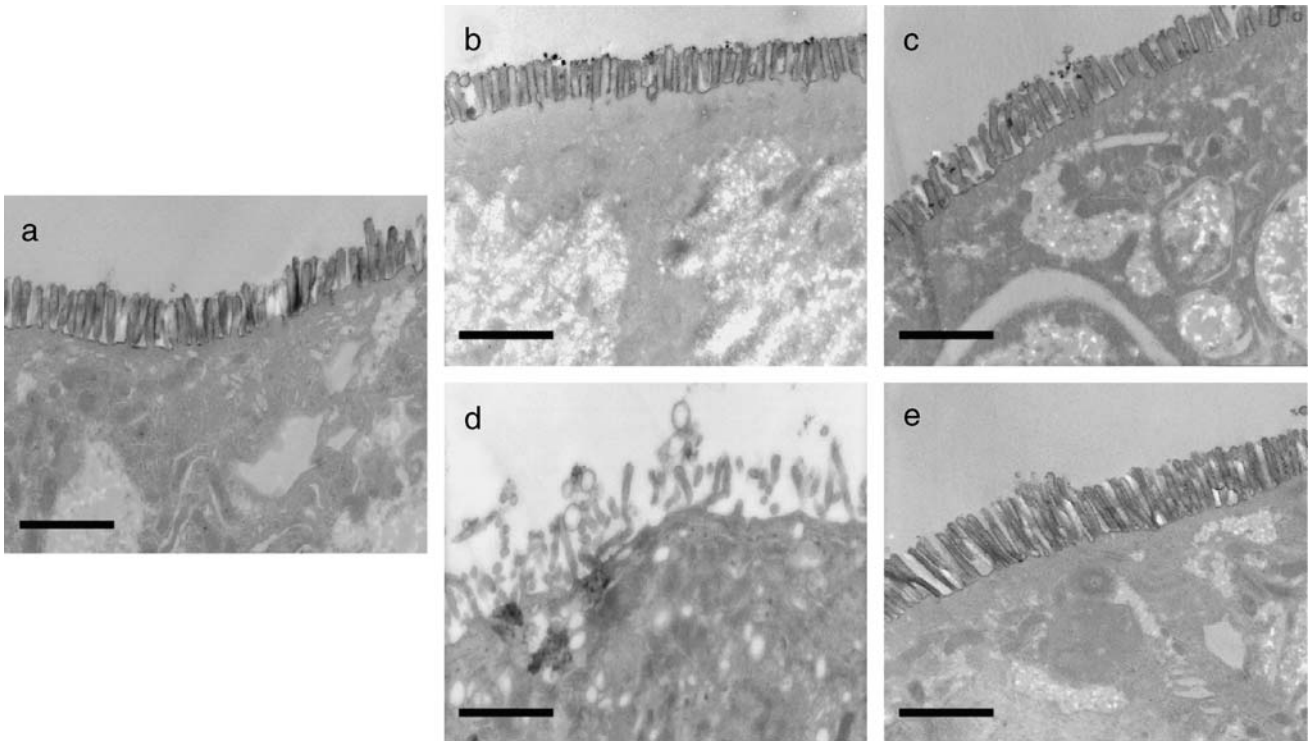

Fig. 5. Transmission electron microscopy (TEM) images of Caco-2 cell monolayers after treatment with PAMAM dendrimers (1 mM) for 2 h: **a** control cells; **b** $G2NH_2$; **c** G1.5COOH; **d** $G4NH_2$; **e** G3.5COOH. The images display a generation-dependent effect of PAMAM dendrimers on Caco-2 microvilli (magnification=12,500×). Scale bars=1 μm.

based drug delivery systems can be tailored to the desired drug delivery application. The increased accumulation of cationic dendrimers in vesicular compartments can be exploited to target anti-cancer agents to tumor cells, which tend to have alkaline vesicular pH (24).

Exposure of epithelial barriers to PAMAM dendrimers affects monolayer integrity causing a reduction in transepithelial electrical resistance (TEER) (5,6,11), and depending on the type of dendrimer, may be a reversible effect (7–9). To explore this phenomenon further, we applied TEM to examine the effect of PAMAM dendrimers on Caco-2 cell monolayer integrity. Untreated, control Caco-2 cells displayed well-differentiated monolayers with intact microvilli (Fig. 5a). This morphology did not change upon treatment with $G2NH_2$ or G1.5COOH (Fig. 5b and c); however, cells treated with $G4NH_2$ dendrimers displayed noticeable cell membrane disruption, as evidenced by a loss of microvilli (Fig. 5d). Additionally, a distortion in monolayer morphology occurred in these cells, a further indication of $G4NH_2$ cytotoxicity. Interestingly, cells treated with anionic dendrimer of similar size (G3.5COOH) were unaffected (Fig. 5e). These findings correspond to our previous cytotoxicity studies in that anionic dendrimers up to G3.5COOH did not significantly reduce cell viability, and had a reversible effect on cell monolayer TEER values (6,8). The effect of $G4NH_2$ dendrimers on microvilli was concentration-dependent, with well-defined microvilli in control cells and at low $G4NH_2$ concentrations (0.01 mM), and an escalation in the disruption and loss of microvilli linear with $G4NH_2$ concentration (Fig. 6a–d). Presumably, for these dendrimers, the greater number of cationic surface groups present in solution increases the interaction with the negatively charged cell membrane when compared to anionic or neutral dendrimers. This, in turn, contributes to the enhanced cytotoxicity of $G4NH_2$ dendrimers. Consistent with these findings other studies have reported hole formation and lipid bilayer disruption caused by cationic dendrimers suggesting that electrostatic interaction between the positively charged den-

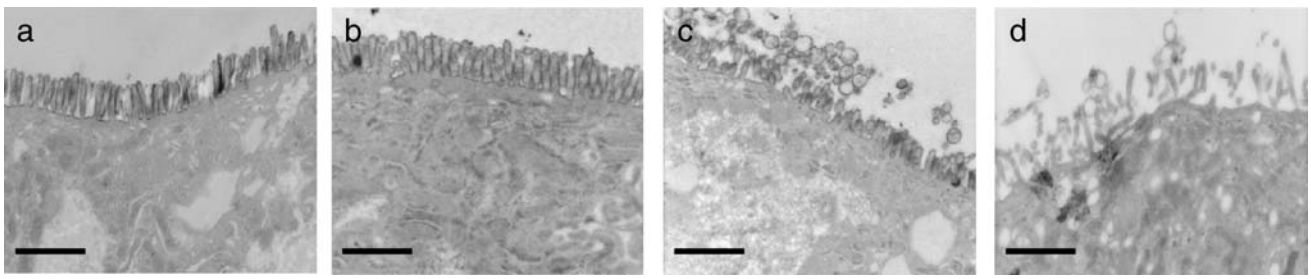

Fig. 6. TEM images of Caco-2 cell monolayers after treatment with $G4NH_2$ dendrimers for 2 h: **a** control cells; **b** 0.01 mM $G4NH_2$; **c** 0.1 mM $G4NH_2$; **d** 1.0 mM $G4NH_2$. The images display a concentration-dependent effect of $G4NH_2$ on Caco-2 microvilli (magnification=12,500×). Scale bars=1 μm.

drimers and negatively charged lipid bilayers may cause internalization of molecules (25–28).

To utilize PAMAM dendrimers as effective oral drug delivery systems, insight into several mechanistic characteristics are of paramount importance: (a) the extent to which these carriers modulate transport; (b) the structural features of the polymer responsible for the enhancement of transport; (c) routes by which transport takes place; and (d) the extent and mechanisms by which the carriers cause cytotoxicity. Confocal microscopy experiments in the present study demonstrate a classical endocytosis pathway for both cationic and anionic dendrimers. Thus, changes in the endosomal microenvironment can be exploited for the design of dendrimer-drug conjugates for intracellular release. For the dendrimers to be effective as oral drug carriers it is also important to cause minimal damage to intestinal cell integrity. Clearly, large cationic dendrimers, when unmodified, have the propensity to cause cellular damage while anionic dendrimers of the same size do not cause disruption of microvilli. This, coupled with previous observations that anionic dendrimers enhance cellular transport, further demonstrate the potential of these carriers in oral drug delivery.

CONCLUSIONS

These studies provide direct evidence that PAMAM dendrimers colocalize with subcellular markers, suggesting endocytosis mechanisms contribute to the internalization and intracellular trafficking of cationic and anionic PAMAM dendrimers across Caco-2 cells. It was further demonstrated that cationic dendrimers likely cause cytotoxicity by compromising the integrity of Caco-2 monolayer microvilli. Intact Caco-2 morphology in the presence of anionic and lower generation, or reduced concentration cationic dendrimers, coupled with evidence of enhanced para- and transcellular transport provide a window of opportunity for the utilization of these probes in oral delivery of poorly bioavailable drugs. The next logical steps are to explore the rate of uptake and transport of dendrimer-drug conjugates with the ultimate goal of selecting carriers for improved *in vivo* oral drug delivery with minimal toxicity.

ACKNOWLEDGEMENTS

The authors thank Dr. Richard Coleman and Maritza Patton for their assistance with the TEM studies. Financial support was provided by a pre-doctoral National Research Service Award from the National Institute of General Medical Sciences (F31-GM67278).

REFERENCES

1. R. Wiwattanapatapee, B. Carreno-Gomez, N. Malik, and R. Duncan. Anionic PAMAM dendrimers rapidly cross adult rat intestine *in vitro*: a potential oral delivery system? *Pharm. Res.* **17**(8):991–998 (2000).
2. K. M. Kitchens, M. E. El-Sayed, and H. Ghandehari. Transepithelial and endothelial transport of poly (amidoamine) dendrimers. *Adv. Drug Deliv. Rev.* **57**(15):2163–2176 (2005).
3. A. D'Emanuele and D. Attwood. Dendrimer-drug interactions. *Adv. Drug Deliv. Rev.* **57**(15):2147–2162 (2005).
4. D. A. Tomalia. Birth of a new macromolecular architechture: dendrimers as quantized building blocks for nanoscale synthetic organic chemistry. *Aldrichimica Acta* **2**(2):39–57 (2004).
5. M. El-Sayed, M. Ginski, C. Rhodes, and H. Ghandehari. Transepithelial transport of poly(amidoamine) dendrimers across Caco-2 cell monolayers. *J. Control. Release* **81**(3):355–365 (2002).
6. M. El-Sayed, M. Ginski, C. A. Rhodes, and H. Ghandehari. Influence of surface chemistry of poly (amidoamine) dendrimers on Caco-2 cell monolayers. *J. Bioact. Compat. Polym.* **18**(1):7–22 (2003).
7. R. Jevprasesphant, J. Penny, D. Attwood, N. B. McKeown, and A. D'Emanuele. Engineering of dendrimer surfaces to enhance transepithelial transport and reduce cytotoxicity. *Pharm. Res.* **20**(10):1543–1550 (2003).
8. K. M. Kitchens, R. B. Kolhatkar, P. W. Swaan, N. D. Eddington, and H. Ghandehari. Transport of poly(amidoamine) dendrimers across Caco-2 cell monolayers: influence of size, charge and fluorescent labeling. *Pharm. Res.* **23**(12):2818–2826 (2006).
9. A. D'Emanuele, R. Jevprasesphant, J. Penny, and D. Attwood. The use of a dendrimer-propranolol prodrug to bypass efflux transporters and enhance oral bioavailability. *J. Control. Release* **95**(3):447–453 (2004).
10. F. Tajarobi, M. El-Sayed, B. D. Rege, J. E. Polli, and H. Ghandehari. Transport of poly amidoamine dendrimers across Madin-Darby Canine Kidney cells. *Int. J. Pharm.* **215**(1–2):263–267 (2001).
11. M. El-Sayed, C. A. Rhodes, M. Ginski, and H. Ghandehari. Transport mechanism(s) of poly (amidoamine) dendrimers across Caco-2 cell monolayers. *Int. J. Pharm.* **265**(1–2):151–157 (2003).
12. J. W. Chen, T. L. Murphy, M. C. Willingham, I. Pastan, and J. T. August. Identification of two lysosomal membrane glycoproteins. *J. Cell Biol.* **101**(1):85–95 (1985).
13. M. M. Manders, F. J. Verbeek, and J. A. Aten. Measurement of co-localization of objects in dual-color confocal images. *J. Microsc.* **169**(3):375–382 (1983).
14. A. R. Hilgers, R. A. Conradi, and P. S. Burton. Caco-2 cell monolayers as a model for drug transport across the intestinal mucosa. *Pharm. Res.* **7**(9):902–910 (1990).
15. R. J. Mrsny. Site-specific drug delivery in the gastrointestinal tract. In K. Park. (Ed.), *Controlled Drug Delivery: Challenges and Strategies*, American Chemical Society, Washington, 1997, pp. 107–123.
16. P. Artursson. Epithelial transport of drugs in cell culture. I: A model for studying the passive diffusion of drugs over intestinal absorptive (Caco-2) cells. *J. Pharm. Sci.* **79**(6):476–482 (1990).
17. S. Yee. *In vitro* permeability across Caco-2 cells (colonic) can predict *in vivo* (small intestinal) absorption in man-fact or myth. *Pharm. Res.* **14**(6):763–766 (1997).
18. C. N. Lok and T. T. Loh. Regulation of transferrin function and expression: review and update. *Biol. Signals Recept.* **7**(3):157–178 (1998).
19. Y. Omidi and M. Gumbleton. Biological membranes and barriers. In R. I. Mahato (Ed.), *Biomaterials for delivery and targeting of proteins and nucleic acids*, CRC Press, Boca Raton, FL, 2005, pp. 231–274.
20. N. R. Gough and D. M. Fambrough. Different steady state subcellular distributions of the three splice variants of lysosome-associated membrane protein LAMP-2 are determined largely by the COOH-terminal amino acid residue. *J. Cell Biol.* **137**(5):1161–1169 (1997).
21. S. L. Schmid, R. Fuchs, P. Male, and I. Mellman. Two distinct subpopulations of endosomes involved in membrane recycling and transport to lysosomes. *Cell* **52**(1):73–83 (1988).
22. D. Langui, N. Girardot, K. H. El Hachimi, B. Allinquant, V. Blanchard, L. Pradier, and C. Duyckaerts. Subcellular topography of neuronal Abeta peptide in APPxPS1 transgenic mice. *Am. J. Pathol.* **165**(5):1465–1477 (2004).
23. I. G. Mills, A. T. Jones, and M. J. Clague. Involvement of the endosomal autoantigen EEA1 in homotypic fusion of early endosomes. *Curr. Biol.* **8**(15):881–884 (1998).
24. A. K. Larsen, A. E. Escargueil, and A. Skladanowski. Resistance mechanisms associated with altered intracellular distribution of anticancer agents. *Pharmacol. Ther.* **85**(3):217–229 (2000).
25. S. Hong, P. R. Leroueil, E. K. Janus, J. L. Peters, M. M. Kober, M. T. Islam, B. G. Orr, J. R. Baker, Jr., and M. M. Banaszak

Holl. Interaction of polycationic polymers with supported lipid bilayers and cells: nanoscale hole formation and enhanced membrane permeability. *Bioconjug. Chem.* **17**(3):728–734 (2006).
26. S. Hong, A. U. Bielinska, A. Mecke, B. Keszler, J. L. Beals, X. Shi, L. Balogh, B. G. Orr, J. R. Baker, Jr., and M. M. Banaszak Holl. Interaction of poly(amidoamine) dendrimers with supported lipid bilayers and cells: hole formation and the relation to transport. *Bioconjug. Chem.* **15**(4):774–782 (2004).
27. A. Mecke, I. J. Majoros, A. K. Patri, J. R. Baker, Jr., M. M. Holl, and B. G. Orr. Lipid bilayer disruption by polycationic polymers: the roles of size and chemical functional group. *Langmuir* **21**(23):10348–10354 (2005).
28. A. Mecke, S. Uppuluri, T. M. Sassanella, D. K. Lee, A. Ramamoorthy, J. R. Baker, Jr., B. G. Orr, and M. M. Banaszak Holl. Direct observation of lipid bilayer disruption by poly (amidoamine) dendrimers. *Chem. Phys. Lipids* **132**(1):3–14 (2004).